

## Replication and transcription sites are colocalized in human cells

A. Bassim Hassan<sup>1\*</sup>, Rachel J. Errington<sup>2</sup>, Nick S. White<sup>3</sup>, Dean A Jackson<sup>1</sup> and Peter R. Cook<sup>1,†</sup>

<sup>1</sup>CRC Nuclear Structure and Function Research Group, Sir William Dunn School of Pathology, University of Oxford, South Parks Road, Oxford OX1 3RE, UK

<sup>2</sup>Department of Zoology, University of Oxford, South Parks Road, Oxford OX1 3PS, UK

<sup>3</sup>Department of Plant Sciences, University of Oxford, South Parks Road, Oxford OX1 3RB, UK

Present address: Department of Medicine, Addenbrookes Hospital, Hills Road, Cambridge CB2 2QU, UK

\*Author for correspondence

### SUMMARY

HeLa cells synchronized at different stages of the cell cycle were permeabilized and incubated with analogues of nucleotide triphosphates; then sites of incorporation were immunolabelled with the appropriate fluorescent probes. Confocal microscopy showed that sites of replication and transcription were not diffusely spread throughout nuclei, reflecting the distribution of euchromatin; rather, they were concentrated in 'foci' where many polymerases act together. Transcription foci aggregated as cells progressed towards the G<sub>1</sub>/S boundary; later they dispersed and

became more diffuse. Replication was initiated only at transcription sites; later, when heterochromatin was replicated in enlarged foci, these remained sites of transcription. This illustrates the dynamic nature of nuclear architecture and suggests that transcription may be required for the initiation of DNA synthesis.

Key words: cell cycle, biotin-dUTP, BrUTP, confocal microscopy

### INTRODUCTION

Sites of replication and transcription in nuclei have been separately labelled with fluorescent probes after incorporation of the appropriate precursors; they are not diffusely spread throughout nuclei reflecting the distribution of 'open' chromatin but concentrated in discrete foci or 'speckles'. For example, when rat fibroblasts are incubated with bromodeoxyuridine and sites of incorporation visualized subsequently using fluorescently labelled antibodies directed against the analogue, ~150 foci - each containing ~20 replication units - can be seen (Nakamura et al., 1986). Similar foci can be labelled with fluorescent streptavidin or antibodies after incorporation of biotin-dUTP by permeabilized cells (Mills et al., 1989; Kill et al., 1991). Analogous transcription sites can also be immunolabelled after incubation with BrUTP (Jackson et al., 1993; see also Wansink et al., 1993) or by hybridization with the appropriate probes (Carter et al., 1993).

We have now localized sites of replication relative to sites of transcription by fluorescence microscopy in synchronized cells. This posed special problems. Firstly, nascent nucleic acids tend to aggregate, making it difficult to ensure that any associations seen are not generated artifactually. Secondly, polymerization occurs so rapidly (i.e. at ~1000 nucleotides/minute) that during incubations long enough for labelling, nascent nucleic acids - especially nascent RNA - have time to move far from their site of synthesis. We minimize these problems by encapsulating living HeLa cells in agarose microbeads (diam ~50 µm), before permeabilizing cell membranes using streptolysin O (Ahnert-Higler et al.,

1989) in a physiological buffer. Under optimal conditions, such permeabilized cells synthesize RNA and DNA at essentially the *in vivo* rate (Jackson et al., 1993; Hassan and Cook, 1993); if complexes containing nascent nucleic acids have aggregated artifactually, they should lose activity. Moreover, encapsulation protects fragile cells and allows thorough washing to remove endogenous pools of triphosphates and unincorporated fluorochromes. Precursor concentrations are adjusted so nascent molecules are elongated by only a few nucleotides; then synthetic - and not more distant - sites are labelled. Cells are also fixed with paraformaldehyde using conditions that preserve the native (i.e. unfixed) pattern of replication foci (Hassan and Cook, 1993), so it is unlikely that these foci are aggregates.

Synchronized cells were encapsulated, permeabilized and incubated with biotin-16-dUTP and BrUTP; these analogues are incorporated specifically into DNA and RNA, respectively (Hozák et al., 1993; Jackson et al., 1993; Hassan and Cook, 1993). After fixation, sites containing incorporated biotin and Br were labelled with different fluorochromes. At the G<sub>1</sub>/S boundary, transcription foci colocalize with replication sites; later, replication foci are larger whilst transcription foci are more diffuse.

### MATERIALS AND METHODS

#### Cell culture and synchronization

Suspension cultures of HeLa cells were grown and synchronized using thymidine and nitrous oxide: cells were first blocked in S-phase

(2.5 mM thymidine; 22 hours), washed, regrown (4 hours) in fresh medium, >95% arrested at mitosis using nitrous oxide at high pressure (8 hours) and regrown in fresh medium (Jackson and Cook, 1986b). The first cells enter S-phase 5 hours after mitosis and G<sub>1</sub>, early S, mid S, late S and G<sub>2</sub> cells were taken 2, 8.5, 13, 18, 20 hours post-mitosis, respectively. Cells were also blocked at the G<sub>1</sub>/S border by adding 5 µg/ml aphidicolin 1 hour post-mitosis and then harvesting 7-9 hours later; then cells were encapsulated in medium containing aphidicolin, washed thoroughly and regrown for 15 minutes without aphidicolin to give G<sub>1</sub>/S cells. In some experiments (not shown) cells were grown for up to 2 hours after removal of aphidicolin; such early S-phase cells gave identical results to those obtained without the aphidicolin block.

### Encapsulation and lysis

Cells were washed 3× in fresh PBS, encapsulated (1-5×10<sup>6</sup> cells/ml) in 0.5% agarose (Jackson et al., 1988) and lysed with streptolysin O (Wellcome; 10 i.u./ml per 10<sup>6</sup> cells; 30 minutes; 4°C) in the physiological buffer (PB) described by Jackson et al. (1993). This contains 22 mM Na<sup>+</sup>, 130 mM K<sup>+</sup>, 1 mM Mg<sup>2+</sup>, <0.3 µM free Ca<sup>2+</sup>, 100 mM CH<sub>3</sub>COO<sup>-</sup> and 30 mM Cl<sup>-</sup>, 11 mM phosphate, 1 mM ATP, 1 mM dithiothreitol and 0.1 mM phenylmethylsulphonyl fluoride (PMSF). Beads were resuspended in an equal vol. of PB and permeabilized (34°C, 2 minutes). All solutions used after lysis were treated with diethylpyrocarbonate to eliminate RNases (Sambrook et al., 1989). In addition, RNasin (Amersham) was added during incubations with antibodies and subsequent washes to final concentrations of 25 and 2.5 units/ml, respectively.

### Replication and transcription

Encapsulated and permeabilized cells were pre-incubated (34°C, 2 minutes), before reactions were started by addition of a 10× concentrated mixture of triphosphates and MgCl<sub>2</sub> to give final concentrations of 0.1 mM CTP, UTP, GTP, dCTP, dATP, dGTP (Pharmacia), 50 µM BrUTP (Sigma), 100 µM biotin-16-dUTP (Boehringer) and 2 mM MgCl<sub>2</sub>. All incubations for fluorescence microscopy were for 10 minutes. For Fig. 1 (below) cells were grown prior to synchronization in [*methyl*-<sup>3</sup>H]thymidine (0.05 µCi/ml; ~60 Ci/mmol) for 18-24 hours to label their DNA uniformly to allow corrections for slight variations in cell numbers, unencapsulated cells were lysed as described above and triphosphate concentrations were altered as follows. In Fig. 1A, 0.1 mM dCTP was replaced by 2.5 µM dCTP plus [<sup>32</sup>P]dCTP (Amersham; ~3000 Ci/mmol; 50 µCi/ml); in some cases BrUTP was replaced by UTP and biotin-dUTP by dTTP. In Fig. 1B, 0.1 mM GTP was replaced by 2.5 µM GTP plus [<sup>32</sup>P]GTP (Amersham; ~3000 Ci/mmol; 50 µCi/ml); in some cases BrUTP was replaced by UTP and biotin-dUTP by dTTP. α-Amanitin and aphidicolin, if present, were incubated (4°C, 15 minutes) prior to lysis and were present during incorporation. Reactions using radiolabel were stopped by removing samples and adding them to 2% SDS; after incubation (2 hours, 37°C), <sup>32</sup>P incorporation into acid-insoluble material was measured by scintillation counting (Jackson and Cook, 1986a).

### Immunolabelling

Incubations for light microscopy were stopped by washing in 10 vol. ice-cold PB. Then nuclear membranes were permeabilized (5 minutes) in ice-cold PB plus 0.5% Triton X-100, washed 4× in PB (10 vol.) and fixed (15 minutes, 4°C) in fresh 4% paraformaldehyde in PB, washed 2× in PB and 2× in PB supplemented with 0.02% Tween-20 (Sigma) and 0.1% BSA. Sites containing incorporated biotin were detected using streptavidin-FITC; those containing Br-RNA were indirectly immunolabelled using a primary antibody raised against a bromodeoxyuridine-BSA conjugate that cross-reacts with Br-RNA and a secondary antibody conjugated with Texas Red (Jackson et al., 1993). Fixed cells were incubated with anti-bromodeoxyuridine (mouse monoclonal, IgG; Boehringer; 2 µg/ml) for (4-16 hours; 4°C), washed 4× with 10 vol. PB+Tween+BSA, then incubated (4-16 hours, 4°C) with sheep anti-mouse Ig, conjugated with Texas

Red (Amersham; 1/1000 dilution) and streptavidin-FITC (Sigma; 0.5 µg/ml; Hozák et al., 1993) and washed 4× with 10 vol. PB+Tween+BSA. Samples (25 µl) were mounted under coverslips in Vectashield (Vector Labs).

Various other antibody combinations were used (conditions during incubations with first and second antibodies, as above); dilutions were adjusted so that there was no cross-reaction with primary or secondary antibodies in double-labelling experiments. (i) Anti-centromere and anti-Sm antibodies (anti-nuclear antigen reference human sera nos 8 and 5; Center for Disease Control, Atlanta; 1/2,000 and 1/20,000 dilutions, respectively) used with FITC- or TRITC-conjugated goat anti-human Fab-specific antibody (Sigma; 1/2000 dilution). (ii) Anti-proliferating cell nuclear antigen (mouse monoclonal IgG; PC-10 of Waseem and Lane (1990) from Oncogene Science; 1 µg/ml) used with sheep anti-mouse Ig, conjugated with Texas Red or fluorescein (Amersham; 1/1000 dilution).

### Fluorescence microscopy

#### Image acquisition

Conventional photographs were taken using a Zeiss Axiophot microscope fitted with an Optivar (1.6×) using Kodak EES colour film (exposures 45-60 seconds), push processed to ASA 1600. Visualization and precise alignment of FITC and Texas Red were achieved using interchangeable excitation filters (DF485 nm, DF575 nm or triple-bandpass, XF56; Omega) with a fixed triple-bandpass dichroic mirror and emission filter (Omega XF56).

Labelled cells were also examined using a Bio-Rad MRC 600 confocal laser-scanning microscope attached to a Nikon Diaphot inverted microscope with an oil-immersion objective (×60; NA 1.4). Simultaneous 3D (x,y,z) images were acquired, using an argon-ion laser (wavelength, 514 nm) of cells double-labelled with FITC and Texas Red (Jackson et al., 1993). The instrument was calibrated using 'Fluoresbrite' carboxylate microbeads (140 and 220 nm diameter; Molecular Probes), which fluoresce in both channels. Generally 8 serial sections were taken for each cell, at intervals of 1 µm; only 1 central slice is shown. Cells were arbitrarily chosen that had significant signal in both channels; 3-5 experiments were carried out for each phase of the cell cycle; ~20 representative cells were analyzed in detail for each phase and typical examples are presented. Data were acquired and processed initially using SOM software (Bio-Rad), then transferred to a Macintosh Quadra for analysis (Adobe PhotoShop and Excel software) before printing by dye-sublimation (Tektronix).

#### Image analysis

Pairs of images were collected simultaneously in the green and red channels; no background due to non-specific binding of antibodies was removed. Intensities were stretched to fill the 256 steps of the grey scale and median filtered (3×3) to give pairs of images (Fig. 2B, below). These were then combined in a 16-bit merge 1; relative intensities in the 2 channels can be determined from the upper look-up tables in Figs 2, 4 (abscissa and ordinate give relative intensities in the 2 channels, respectively). A notional line (25 µm long) was then drawn across merge 1 (or merge 3; see below) from the large arrowhead to the small arrowhead; green and red lines in the resulting graph give intensities (ordinate; 0-100%) along the line relative to the brightest focus in each channel in each nucleus.

A reasonable threshold was selected as follows (see also Taneja et al., 1992). Intense foci are analogous to peaks (signal) rising above a plain (background). A high threshold was set and progressively reduced; foci initially expanded slowly in size as the threshold slid down the steep sides of peaks and when it passed an inflexion point just above the valley floor (i.e. background), signal suddenly filled the nucleus. The reasonable threshold for each channel was selected on average 25 steps (range 20-38) above the inflexion point on the 256-step scale and includes all signal that is morphologically significant. Thresholds for green and red channels were within 5 steps of each

other; the average is indicated by the blue line in each graph. Next, all pixels with values above this threshold were assigned the values 1 (green channel) and 2 (red channel); then the resulting images were added together and pixels with values of 1, 2 and 3 were assigned the pseudo-colours of green, red and blue, respectively. In the resulting simplified colocalization image (merge 2), green and red indicate areas where replication and transcription occur alone, whilst blue (equivalent to the binary operation green AND red) indicates areas where they occur together, irrespective of their intensity above the threshold. This threshold excludes the bottom ~10% of signal but includes nearly all morphological information, since coloured areas in merge 2 are larger than bright areas in the corresponding merge 1. There are a series of merge 2 images, each with different reasonable thresholds, but only one is presented.

Colocalization information (i.e. blue in merge 2) was then combined with intensity information contained in the corresponding merge 1. In such a 24-bit 3-channel display (merge 3), white represents regions rich in both (blue) FITC (green) and Texas Red (red); areas where the two are colocalized, but the two signals have different intensities, appear a shade of blue, as indicated in the lower look-up tables in Figs 2 and 4 (below).

Quantifying the degree of coincidence of two complex - and ever-changing - patterns is difficult (e.g. see Taneja et al., 1992). We especially wanted to distinguish true from spurious colocalization due to randomly distributed transcription foci (i.e. a complex pattern) lying above or below replication foci (a simple or complex pattern, depending on the stage of the cycle). Therefore, we adopted a comparative approach that relied on simple morphological assumptions and that maximized coincidence of peaks in two non-overlapping complex patterns; then if a higher level of coincidence is seen, it is likely to be real. The summit of the brightest peak in one channel was selected and the distance in pixels to the nearest summit (the target) in the other channel, which is not necessarily in the highest peak, determined; then the next brightest was selected and so on. A summit is defined as any pixel (occasionally a group of pixels of equal intensity) at least one step above all surrounding pixels. (Definitions involving summits with more adjacent pixels or steps above surroundings introduce additional assumptions about focus shape and minimize overlap between non-overlapping complex patterns.) The process was then repeated, beginning with the brightest peak in the other channel. All peaks selected were >50% as bright as the brightest in that channel. Points ~200 nm apart in a single channel can be resolved by Rayleigh criteria, so relative positions of peaks in a single channel can be determined to within a pixel provided they are further apart than 200 nm. The relative positions of peaks in separate channels can always be determined to within a pixel, which in our case is 70 nm (Shaw et al., 1992). Non-overlapping but complex patterns were created artificially by superimposing a (red) transcription pattern collected from a G<sub>1</sub> cell onto a (red converted to pseudo-green) transcription pattern from a G<sub>2</sub> cell (labelled T\* > T\* and T\* < T\* in Table 1, below). Superimposing a (simpler) replication pattern from one cell on to the transcription pattern of another creates even less random overlap.

### Specificity of labelling

Controls demonstrated specificity of labelling and that there was no cross-labelling of DNA by BrUTP or RNA by biotin-dUTP, or bleed-through between channels. (For additional controls after labelling singly with BrUTP or biotin-dUTP see Jackson et al. (1993), Hozák et al. (1993) and Hassan and Cook (1993).) Labelling levels were adjusted so that there was no detectable nuclear signal above noise in the appropriate channel if either BrUTP or biotin-dUTP was omitted during incubation with triphosphates. Hence the Texas Red signal was always strong enough such that bleed-through from the FITC channel was undetectable. Lack of bleed-through from red to green channel is illustrated by G<sub>1</sub> and G<sub>2</sub> cells in Fig. 3. Additional biological controls using simple and complex patterns, inhibitors, RNase A (Sigma) and DNase I (Boehringer; RNase-free) are described for Figs 2 and 5 (below).

## RESULTS

### The effects of triphosphate analogues on nucleic acid synthesis

We first measured rates of DNA and RNA synthesis in the presence of biotin-16-dUTP and BrUTP. Using the natural precursors and a limiting concentration of dCTP with [<sup>32</sup>P]dCTP as a tracer, radiolabel is initially incorporated at ~40% of the rate found in vivo (Fig. 1A, curve 1). Replacement of UTP by BrUTP has no effect on this DNA synthesis (Fig. 1A, curve 2), whereas replacement of dTTP by biotin-dUTP reduces incorporation to ~7% of the in vivo rate (Fig. 1A, curve 3) and, again, BrUTP has no further effect (Fig. 1A, curve 4). Aphidicolin (which inhibits DNA polymerase  $\alpha$ ) prevents this DNA synthesis (Fig. 1A, curve 5), but 250  $\mu$ g/ml  $\alpha$ -amanitin (which inhibits RNA polymerase II) has no effect (not shown).

The analogous experiment - using natural precursors and a limiting concentration of GTP with [<sup>32</sup>P]GTP as a tracer - shows how radiolabel is incorporated into RNA (Fig. 1B, curve 1). Replacement of UTP by BrUTP slightly reduces the rate (Fig. 1B, curve 2), but then replacement of dTTP by biotin-dUTP has no further effect (Fig. 1B, curve 3).  $\alpha$ -Amanitin at 250  $\mu$ g/ml further reduces incorporation (Fig. 1B, curve 4); most remaining synthesis is due to polymerase I, which is inhibited by 1000  $\mu$ g/ml  $\alpha$ -amanitin (Fig. 1B, curve 6) but not by aphidicolin (Fig. 1B, curve 5).

We routinely incubate for 10 minutes in both biotin-dUTP and BrUTP. As permeabilized cells do not initiate, and if DNA synthesis occurs in vivo at 50 nucleotides/second (Kornberg and Baker, 1992) and there are ~35,000 active RNA polymerases per cell (Cox, 1976), then nascent DNA and RNA chains will be extended by ~2000 and ~400 nucleotides, respectively. Therefore polymerization sites will be labelled rather than distant processing sites.

### Simultaneous visualization of replication and transcription sites

Replication sites (containing incorporated biotin) were labelled using streptavidin tagged with FITC, and transcription sites (containing incorporated Br) with an anti-Br-RNA antibody, followed by a second antibody tagged with Texas Red. Labelled cells were photographed using a conventional camera; FITC fluorescence reveals sites of replication (Fig. 2A, green nuclei). The two nuclei have patterns typical of early S-phase (i.e. dispersed foci) and mid S-phase (i.e. peripheral foci; e.g. see O'Keefe et al., 1992). Texas Red fluorescence of the same two cells reveals sites of transcription spread throughout extranucleolar regions (Fig. 2A, middle). Many foci in these round nuclei lie above and below the focal plane, generating out-of-focus flare; then individual foci are best seen at the periphery. When photographed through a triple-bandpass filter that allows precise alignment of red and green fluorescence, some intense green foci are seen to colocalize with red foci, giving orange against a red background (Fig. 2A, bottom).

### Image processing

The complexity of these images and background flare makes analysis of the extent of colocalization difficult. Confocal microscopy removes out-of-focus flare and facilitates quantitative analysis. Colocalization information is generally

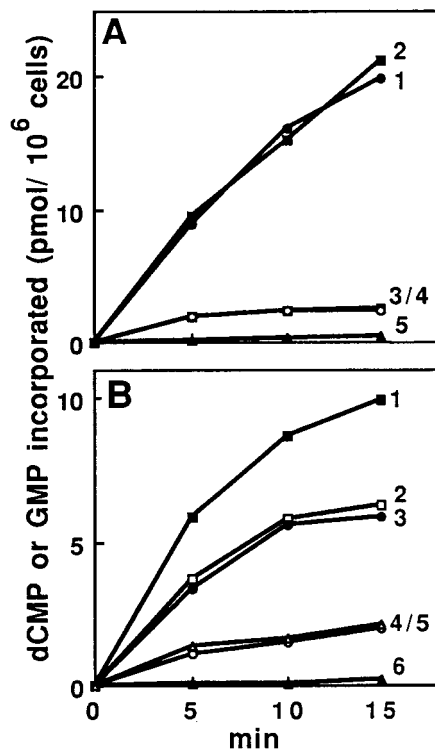


**Fig. 1.** Effects of various analogues on (A) replication and (B) transcription by permeabilized HeLa cells. (A) Replication rates were measured by incorporating [ $^{32}$ P]dCTP into acid-insoluble material in the presence of 100  $\mu$ M dTTP or biotin-dUTP and 50  $\mu$ M UTP or BrUTP: (1) dTTP and UTP; (2) dTTP and BrUTP; (3) biotin-dUTP and UTP; (4) biotin-dUTP and BrUTP; (5) biotin-dUTP, BrUTP and 5  $\mu$ g/ml aphidicolin. (B) Transcription rates were measured by incorporating [ $^{32}$ P]GTP into acid-insoluble material as for (A): (1) dTTP and UTP; (2) dTTP and BrUTP; (3) biotin-dUTP and BrUTP; (4) biotin-dUTP, BrUTP and 250  $\mu$ g/ml  $\alpha$ -amanitin; (5) biotin-dUTP, BrUTP and 250  $\mu$ g/ml  $\alpha$ -amanitin and 5  $\mu$ g/ml aphidicolin; (6) biotin-dUTP, BrUTP, 1000  $\mu$ g/ml  $\alpha$ -amanitin.

presented by merging all intensity information from both channels or just that above a reasonable threshold (e.g. see Taneja et al., 1992); we combine these merges in turn to obtain both intensity and colocalization information in a single image.

Our approach is illustrated in Fig. 2B, in which a simple pattern (given by centromeres labelled with FITC) is compared with a (non-overlapping) complex pattern (given by proliferating cell nuclear antigen, PCNA, labelled with Texas Red). Pairs of images of an optical slice through the centre of a single cell were collected simultaneously using a single excitation wavelength and appropriate filters to separate the two emission signals, and combined to give merge 1; the red and green patterns hardly overlap. (Yellow indicates overlap; see look-up table, top right.) Merge 1 has a limited colour range and weak signals tend to go unnoticed.

When analyzing complex patterns it is often difficult to determine signal from background. Therefore only signals above a reasonable threshold - indicated by the blue line in graph (see below) - were made pure green or red. The resulting merge 2 shows areas where signal is above this threshold in one channel (green or red) or in both (blue); it contains mor-

phological information irrespective of intensity. Colocalization information (i.e. blue in merge 2) was then recombined with intensity information in merge 1 to give merge 3. Areas where the two are colocalized above the threshold appear blue-white and their respective intensities can be determined from a look-up table (Fig. 2B, bottom right). The centromeric and PCNA patterns are clearly different (i.e. in merge 3, many sites are green or red and few are blue-white). Intensities in the two channels along an imaginary line drawn through the large arrowhead to the small arrowhead in merge 3 are given in the adjacent graph; the (green) profile across the discrete centromeres is spiky, compared to that (in red) across diffusely spread PCNA.

### Biological colocalization standards

We next analyzed pairs of identical patterns of increasing complexity (i.e. centromere/centromere, PCNA/PCNA, and Sm antigen/Sm antigen); all merge 3 images appear blue-white and the two lines in the graphs are largely coincident (Fig. 2C). These provide standards for comparison with test patterns, the simple centromeric pattern being roughly similar to the late-replication pattern, the intermediate PCNA pattern to the replication and transcription patterns found early during S-phase and the complex Sm pattern to the transcription pattern seen during G<sub>1</sub> and G<sub>2</sub>. (Fig. 2D is discussed below.)

### Changes in replication patterns

Primary images of optical slices through six different cells, each at a different phase of the cell cycle, are illustrated in the six rows in Fig. 3; processed images are presented in the corresponding rows in Fig. 4. In Fig. 3, the first image of the pair illustrates sites of biotin incorporation and so replication (column R). No incorporation occurs during G<sub>1</sub>. At the G<sub>1</sub>/S boundary small foci appear and by mid S-phase they are larger and concentrated around nucleoli and the nuclear periphery; later, foci become very large, to disappear in G<sub>2</sub> (see also Nakamura et al., 1986; Nakayasu and Berezney, 1989; O'Keefe et al., 1992). (Note that nucleoli appear as black holes.)

### Changes in transcription patterns

Sites of BrUMP incorporation (i.e. transcription) also change shape (Fig. 3, column T); a diffuse network throughout extranucleolar regions condenses at the G<sub>1</sub>/S boundary into punctate foci, to disperse within 1 hour (not shown). These transitions are reflected by the graphs in Fig. 4. The red line in the G<sub>1</sub> graph rises relatively smoothly to the mid-point and then falls, whereas in the G<sub>1</sub>/S and ES graphs it is spikier, reminiscent of profiles across discrete centromeres in Fig. 2B,C; graphs for MS, LS and G<sub>2</sub> cells are again smoother between the peaks in LS and G<sub>2</sub>, which are probably due to coiled bodies (see later).

### Replication and transcription sites colocalize early during S-phase

Inspection of the merges in Fig. 4 show that replication and transcription are tightly colocalized at the G<sub>1</sub>/S boundary and early during S-phase. As there is no replication in G<sub>1</sub>, all merges appear red. (Merges 1 and 3 are identical, so only merge 3 is shown.) At the G<sub>1</sub>/S boundary, widely-spread red (transcription) sites of G<sub>1</sub> draw together to underlie new green (replication) sites, giving yellow in merge 1; merge 2 images

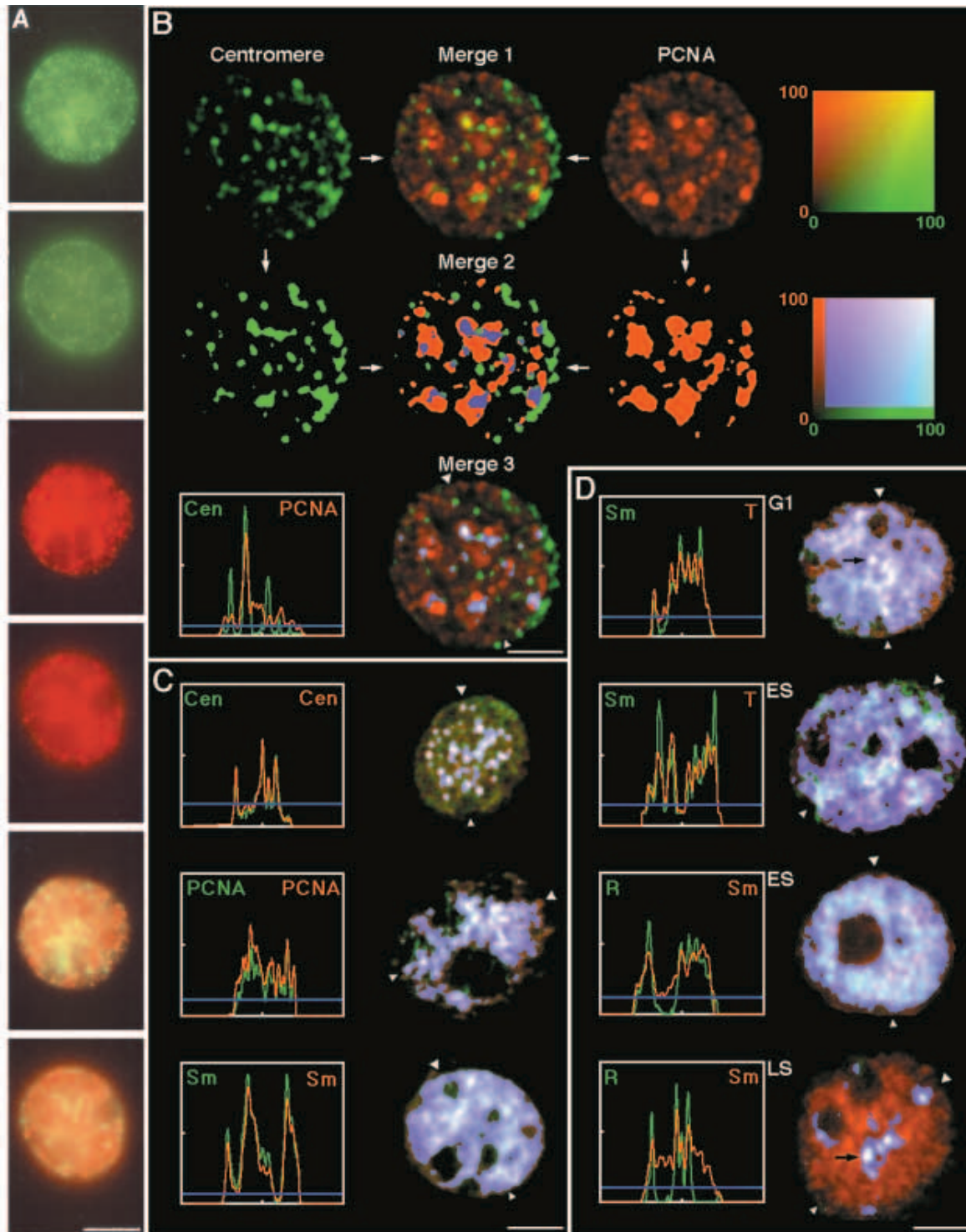


**Fig. 2.** Colocalization of various sites. Bars, 5  $\mu\text{m}$ . (A) Sites of replication and transcription. Unsynchronized and permeabilized cells were incubated with biotin-dUTP and BrUTP for 10 minutes and sites of incorporation labelled with FITC (biotin-dUTP) and Texas Red (BrUTP). Colour photographs of the same two cells were taken using a triple-bandpass filter and a conventional microscope. Upper pair (green channel): sites containing FITC (replication). Middle pair (red channel); sites containing Texas Red (transcription). Lower pair (both channels): sites containing both (replication and transcription). (B) Steps in the processing of images collected by confocal microscopy. PCNA is distributed in a mid/late S-phase replication pattern and the bright white focus in merge 3 may contain a replicating centromere (O'Keefe et al., 1992; Vourc'h et al., 1993). The bottom look-up table should be used to determine colocalization in merge 3 images in C and D. (C) Graphs and merge 3 images illustrating colocalization of centromeres, PCNA or Sm with themselves. Unsynchronized cells were indirectly labelled using a single first antibody (anti-cen, anti-PCNA or anti-Sm) and a mixture of a secondary antibody conjugated with a green fluorochrome (FITC or fluorescein) plus the same antibody conjugated with a red fluorochrome (TRITC or Texas Red). (D) Graphs and merge 3 images illustrating colocalization of sites containing Sm antigen and sites of transcription (T) or replication (R) in cells from G<sub>1</sub>, early S (ES) or late S-phase (LS).

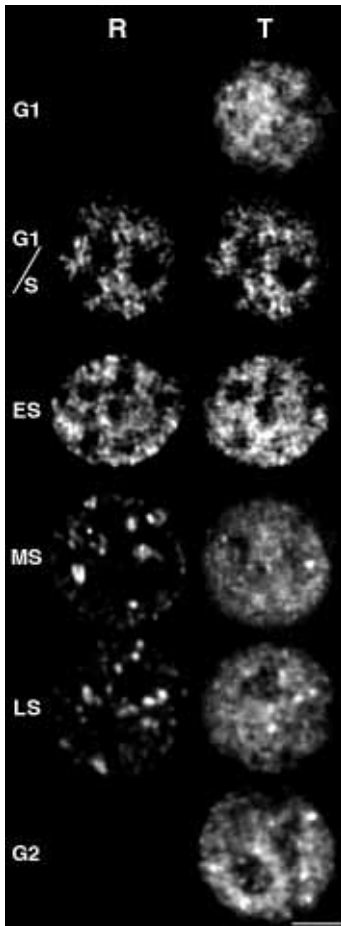


**Fig. 3.** Sites of replication (R) and transcription (T) in synchronized cells from G<sub>1</sub>, G<sub>1</sub>/S, early, mid and late S-phase (ES, MS and LS, respectively) and G<sub>2</sub>. A pair of primary images of one confocal section were collected using green and red filters for each of six cells. Bar, 5 µm.

are largely blue and merge 3 images blue-white, indicating colocalization. Little replication or transcription occur alone (which would appear green or red).

#### Are late-replicating regions also transcribed?

Heterochromatin, which is usually assumed to be transcriptionally inert, is replicated during mid or late S-phase (e.g. see Hatton et al., 1988; O'Keefe et al., 1992), so we might expect most replication sites to be free of transcription and so green in the merges in Fig. 4. Although some areas are green in merge 1, the most intense appear blue in merge 2 or blue-white in merge 3, indicating that they are sites of both replication and transcription, contrary to expectation. There is little bright green in any merge 3 image; intense replication does not occur in the absence of transcription at any stage. Whilst some green areas in merge 2 (e.g. arrows 1-4 in MS) suggest peripheral heterochromatin is replicated at transcription-free sites, merges 1 and 3 show they appear green only because weak replication and transcription signals lie, respectively, just above and below the arbitrary threshold. Others, like the green nucleolar focus in LS merge 1 (arrow 6), have higher levels of transcription and appear blue in merge 3. The most intense green focus seen in any merge 3 is at the periphery of the LS image (arrow 5) and is perhaps a replicating centrosome.

#### Comparison with biological colocalization standards

Replication and transcription foci are ~250 nm in diameter and

our confocal sections are ~1 µm thick so some transcription foci might lie above or below replication foci, fortuitously appearing to colocalize with them. If foci are randomly distributed, peak intensities should rarely coincide; if truly colocalized, peaks should coincide to the same extent as those in the biological standards. This comparative approach exploits the better *x,y* resolution of the confocal microscope and eliminates any systematic errors in image acquisition or processing; it also requires few arbitrary assumptions concerning focus shape, intensity or threshold and allows results from different cells to be pooled.

For each marker pair, the brightest peak in one channel was selected and the distance to the nearest peak in the other channel measured; then the next brightest was selected and so on down to the tenth brightest before results from five different cells were pooled. Then the process was repeated after selecting the brightest peak in the other channel, giving two sets of data for each marker pair (indicated in Table 1 by marker1>marker2 and marker1<marker2). Doubly labelled plastic beads with diameters roughly the size of foci give the values of perfectly colocalized fluorochromes; peaks are not exactly coincident, reflecting the limits of the system (Table 1, beads>beads and beads<beads). Single markers labelled with both fluorochromes provide another series of overlapping patterns (Table 1, overlapping patterns). As the complexity of the pattern increases, the peak-to-peak dispersion increases. PCNA and centromeric patterns provide an extreme case of random colocalization given by non-overlapping patterns (PCNA>cen and PCNA<cen). This spurious colocalization increases as the complexity of the non-overlapping patterns increases; an example involving the most complex patterns analyzed is given (i.e. where the transcription pattern of one cell overlies that of another cell; T\* > T\* and T\* < T\*). Any overlap of experimental patterns that is greater than this random colocalization is likely to be real.

Inspection of Table 1 confirms the qualitative impressions gained earlier. For example, 100% Sm peaks in one channel lie within 4 pixels of an Sm peak in the other (Table 1, Sm>Sm and Sm<Sm); 4 pixels provide a convenient distance for comparison. Values for T<R are all above the 24% given by the random colocalization of two complex patterns (i.e. T\* > T\* and T\* < T\*). The highest values are found at the G<sub>1</sub>/S boundary, but even so the overlap is not as good as that found between Sm and itself, implying that closely associated sites are not so perfectly intermingled. Indeed, both signals frequently fill a focus of 10-20 pixels, with each being concentrated in different distinct regions (not shown); however, confirmation of this impression awaits more sophisticated analysis. Note also that at the G<sub>1</sub>/S boundary, values for T>R and T<R are roughly equivalent. Later, values diverge, indicating that some transcription sites are separate from replication sites.

#### Controls

Various biological controls show there is no bleed-through between the two channels during image collection or processing. For example, mitotic cells give no signal in either channel (not shown) and there is no FITC signal (replication) in G<sub>1</sub> or G<sub>2</sub> cells (Fig. 3R). Moreover, RNase treatment reduces the intensity of transcription foci, but not replication foci (Fig. 5A,B) whilst DNase has the opposite effect (Fig.

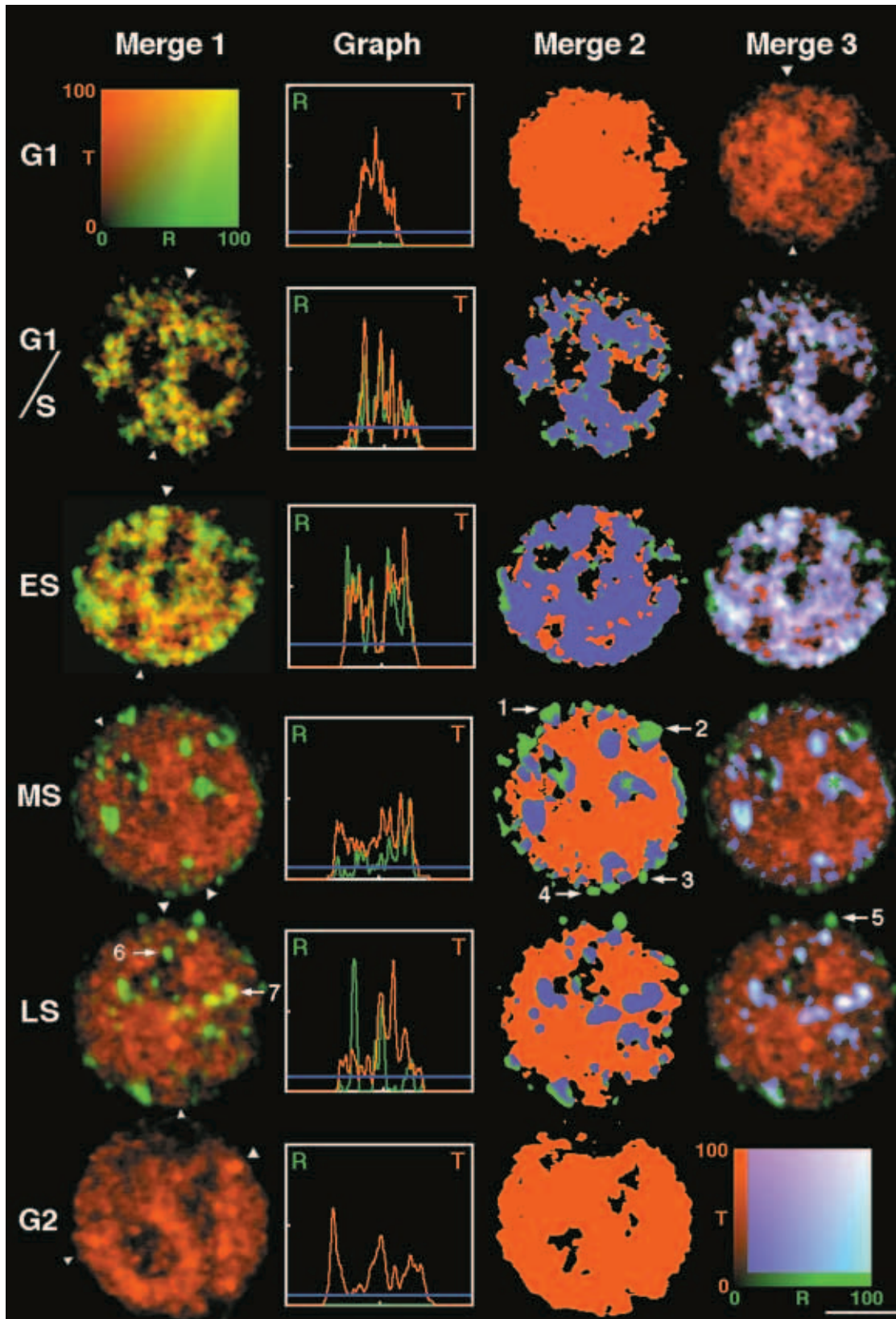


**Fig. 4.** Colocalization of replication and transcription sites. The six pairs of images in Fig. 3 were processed to give merges and graphs in the corresponding row of Fig. 4. Merges 1 and 3 of G<sub>1</sub> and G<sub>2</sub> cells were identical, so only one is shown. Look-up tables at top left and bottom right should be used for merges 1 and 3, respectively. Bar, 5 μm.

5C,D); a combined treatment reduces the intensity of both, aggregating residual foci (Fig. 5E,F; see also Jackson and Cook, 1988). (DNase and RNase generally removed almost

all replication and transcription foci from unsynchronized cells (Jackson et al., 1993; Hozák et al., 1993; Hassan and Cook, 1993) whereas the 10× higher concentration used here

**Table 1. Colocalization of peaks of replication and transcription relative to 'biological' standards**

Marker	Cell cycle phase	% Peaks lying within given no of pixels of each other					
		0	1	2	3	4	>4
Beads>beads (140 nm)	–	36	84	100			
Beads<beads (140 nm)	–	36	84	100			
Beads>beads (220 nm)	–	32	78	100			
Beads<beads (220 nm)	–	32	78	100			
Overlapping patterns							
cen>cen	Random	54	96	100			
cen<cen	Random	54	96	100			
PCNA>PCNA	Random	36	68	94	100		
PCNA<PCNA	Random	36	68	94	100		
Sm>Sm	Random	38	72	94	98	100	
Sm<Sm	Random	38	72	94	98	100	
Experimental patterns							
T>R	G <sub>1</sub> /S	12	32	52	66	78	100
T<R	G <sub>1</sub> /S	14	30	50	72	82	100
T>R	ES	2	4	18	24	34	100
T<R	ES	6	16	32	56	66	100
T>R	MS	0	6	14	32	44	100
T<R	MS	2	22	40	62	72	100
T>R	LS	2	16	20	26	42	100
T<R	LS	2	12	18	30	42	100
Non-overlapping patterns							
T* > T*	G <sub>1</sub> +G <sub>2</sub>	0	2	10	16	24	100
T* < T*	G <sub>1</sub> +G <sub>2</sub>	0	2	8	12	24	100
PCNA > cen	Random	2	2	2	4	4	100
PCNA < cen	Random	6	8	8	10	10	100

Marker pairs were labelled with FITC and Texas Red and the distance in pixels (1 pixel is 70 nm<sup>2</sup>) from the 10 brightest peaks in the red channel to the nearest peaks in the green channel determined (indicated by marker>marker). Pooled results from 5 different cells (i.e. for 50 foci) or for 50 beads are expressed as a percentage of peaks lying within the distance indicated. The experiment was repeated after selecting the brightest focus in the green channel (indicated by marker<marker). Markers: 140 and 220 nm diameter beads, centromere (cen), PCNA, Sm antigen, replication (R), transcription (T) and an artificial non-overlapping complex pattern (T\* > T\* and T\* < T\*).

with these early S-phase cells did not, perhaps because their foci are so dense (Hozák et al., 1993.) Aphidicolin eliminates incorporation into replication foci (Fig. 5G) but not transcription foci (Fig. 5H). Conversely, 250 µg/ml α-amanitin has no effect on replication (Fig. 5I) but reduces extranucleolar transcription to low levels without affecting nucleolar transcription (Fig. 5J; nucleoli, which appear as the large black holes in Fig. 5I, contain the bright foci). Merging the images in Fig. 5I and J shows that most transcription within replication foci - but not all - is abolished by α-amanitin, confirming that it is due to RNA polymerase II. α-Amanitin (at 1000 µg/ml) inhibits nucleolar transcription, but again has no effect on the residual extranucleolar activity (not shown; see also Fig. 1B).

### Colocalization of foci with sites containing Sm antigen

Sm antigen - a component of the splicing machinery - colocalizes with transcription sites (Jackson et al., 1993), so it was of interest to see if it, too, colocalized with replication sites. The examples in Fig. 2D show that Sm antigens underlie both transcription and replication sites (i.e. give blue in merge 3).

Sm antigens are also concentrated in coiled bodies, which are easily recognized as discrete and intensely fluorescent

circles (Carmo-Fonseca et al., 1993). These are variably transcribed during the cycle; for example, one is actively transcribed in G<sub>1</sub> (Fig. 2D, Sm/T-G<sub>1</sub>; arrow). They are also replicated both early and late in S-phase (e.g. Fig. 2D, R/Sm-LS, arrow). (Analogous bright circles in Fig. 3 column T, MS, LS, G<sub>2</sub> and Fig. 4 LS (arrow 7) are probably also coiled bodies.)

## DISCUSSION

When permeabilized cells are incubated with biotin-dUTP and BrUTP, the analogues are incorporated into sites where DNA and RNA are synthesized; subsequently these sites were simultaneously immunolabelled with FITC and Texas Red. When viewed down a conventional microscope through a filter that allowed precise alignment of red and green fluorescence, some replication foci appeared to colocalize with transcription sites (Fig. 2A).

### Comparative imaging

The extent of colocalization of these foci was then analyzed by confocal microscopy. It is important to stress the technical limitations of this instrument when analyzing foci with diameters of ~250 nm. Points ~200 nm apart in the xy plane can be resolved, but resolution in the z axis is poorer (i.e. ~500 nm). z axis resolution can be improved by digitally deconvoluting

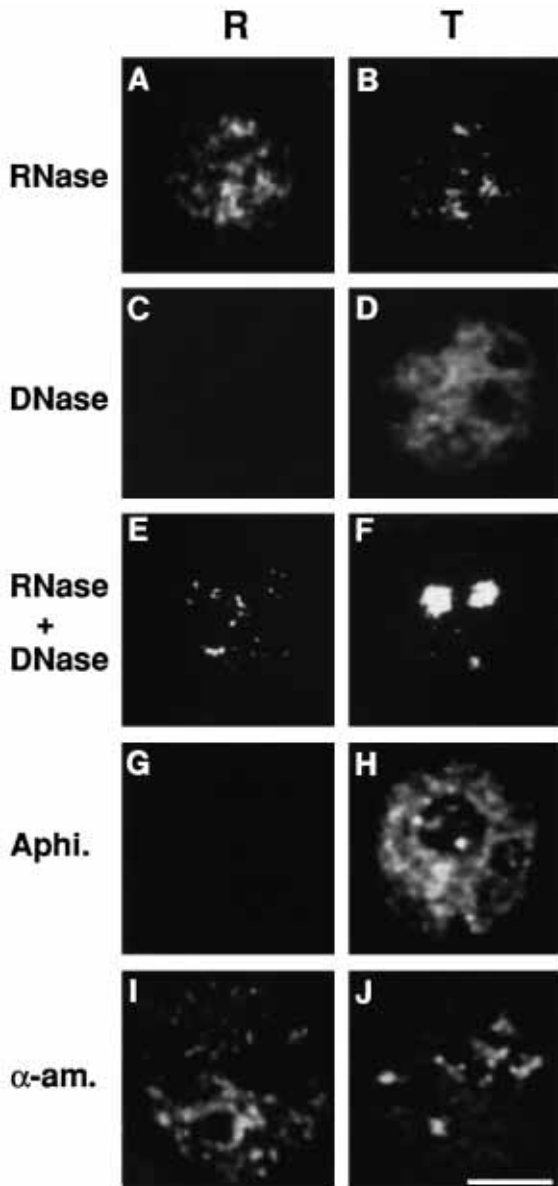


**Fig. 5.** The effects of pretreatments on replication (R; FITC) and transcription (T; Texas Red) in early S-phase cells. A pair of primary images of one confocal section are illustrated in the five rows. Some samples were treated (30 minutes; 34°C) with 250 units/ml RNase and/or 58 units/ml DNase after incorporation but prior to fixation; others were treated with 5 µg/ml aphidicolin (Aphi.) or 250 µg/ml  $\alpha$ -amanitin ( $\alpha$ -am.) prior to (15 minutes; 4°C), and during, incorporation. Bar, 5 µm.

information from serial sections, but this brings attendant problems (e.g. see Shaw et al., 1992). Therefore, we analyzed single central sections and relied on additional morphological information to determine whether sites colocalize. We exploit the better resolution in the *xy* plane and assume that if green and red signals have the same complex shapes they must emanate from the same place; this morphological information is given in the various merges. The extent of colocalization in experimental samples was then gauged relative to biological standards in which simple and complex patterns were colocal-

ized both with themselves and with each other (Fig. 2B,C; Table 1). Ultimately we hope to put confidence limits on the degree of colocalization, but this requires further sophisticated analysis including, for example, effects of object orientation and signal attenuation (e.g. see Taneja et al., 1992; Manders et al., 1993).

### A transcription cycle

Primase-dependent RNA synthesis is required during replication for primer synthesis but this is tiny relative to incorporation due to other RNA polymerases. ~80% synthesis is sensitive to 250 µg/ml  $\alpha$ -amanitin, whilst much of the rest is inhibited by 1000 µg/ml (Figs 1B and 5), so most extranuclear incorporation is due to RNA polymerase II and nucleolar activity to polymerase I (Kornberg and Baker, 1992).

As others have found (e.g. see Nakamura et al., 1986; Nakayasu and Berezney, 1989), replication initiates in ~150 foci whilst those in mid-S-phase are concentrated around nucleoli and the nuclear periphery; later they are still larger, before disappearing in G<sub>2</sub> (Fig. 3). This replication cycle runs in parallel to a transcription cycle: in G<sub>1</sub>, ~300 transcription sites are diffusely spread throughout nuclei, which - on entry into S-phase - aggregate into ~150 foci to disperse later to re-establish the original pattern (Fig. 3). This highlights how dynamic nuclear structure is.

### Colocalization of replication and transcription sites

Nearly all transcription sites aggregate late in G<sub>1</sub> to underlie emerging replication sites; later during S-phase, sites dedicated solely to transcription re-emerge (Fig. 4). RNA polymerase II is responsible for most transcription in replication foci as it can be inhibited by  $\alpha$ -amanitin (Fig. 5I,J). (We cannot exclude the possibility that an  $\alpha$ -amanitin-insensitive activity (e.g. RNA polymerase III) is responsible for some transcription in replication foci (Fig. 5I,J).) Of course, at the molecular level, sites of replication and transcription cannot colocalize perfectly - a nucleotide cannot be replicated and transcribed simultaneously - but at the resolution of the light microscope the colocalization is clearly greater than the random colocalization given by two complex patterns (Table 1).

To what extent are late-replicating sites (i.e. during mid and late S-phase) free of transcription? As these sites are heterochromatic, we might expect them to be transcriptionally inert (e.g. see Hatton et al., 1988; O'Keefe et al., 1992). Then the (simple) late-replicating pattern should only slightly overlap the (complex) transcription pattern, perhaps only to the limited extent seen between the simple centromeric pattern and the complex PCNA pattern; however, the overlap is greater (Table 1). Most highly active replication sites are also transcribing; no intense green (i.e. intense replication occurring in regions with low transcription) is visible in Fig. 4, merge 3. Whether sites of lower replicational activity are also transcribed - and whether replication can ever take place in the complete absence of any transcription - must await further study.

### Dependence of initiation of DNA synthesis on transcription

These results beg the question: is there a functional relationship between replication and transcription foci? Electron microscopy shows each early S-phase replication focus, which contains ~20 active replicons, to be a dense ovoid structure (diam. ~175 nm)

attached to a nucleoskeleton; nascent DNA is extruded from the ovoid as it is made (Hozák et al., 1993; see also Cook, 1991). Presumably, transcripts are made in analogous factories (Jackson et al., 1993; Xing et al., 1993). Then we might imagine that replication factories are assembled around ~20 origins into an ovoid. As this will occur initially in open chromatin, transcription sites will inevitably be caught up in the associated structural reorganization. When DNA synthesis in these replicons is complete, duplicated DNA and associated transcription sites will be released. Only later will heterochromatic regions be replicated. According to this view, transcription sites play a role in opening chromatin, but are then passively dragged along by the template movements required for replication.

Our results are also consistent with a more direct involvement of RNA polymerase II and/or III in replication. As DNA synthesis continues in the presence of  $\alpha$ -amanitin both in vitro (see discussion of Fig. 1A; Fig. 5I) and in vivo (Adolph et al., 1993), RNA polymerase II is not required for replicational elongation; however, the striking colocalization of sites at the G<sub>1</sub>/S border (Fig. 4, Table 1) and the inhibition by  $\alpha$ -amanitin of entry into S-phase (Adolph et al., 1993) suggest that transcription might play a role during initiation. There is evidence both for and against this in other organisms. For example, the inhibitor of bacterial transcription, rifampicin, prevents initiation in vitro at *oriC* and all other known origins are close to transcription units and/or sites where transcription factors bind (e.g. see Kornberg and Baker, 1992; Heintz, 1992); then transcription might be required to seed assembly of replication factories. On the other hand,  $\alpha$ -amanitin does not inhibit the early development of *Drosophila* or *Xenopus*, when replication occurs without detectable transcription (e.g. see Edgar and Schubiger, 1986; Newport and Kirschner, 1982). However, the high concentration of endogenous enzymes and triphosphates in such embryos complicates interpretation; moreover, quite different demands are made on the replication machinery in mammalian cells in tissue culture. Therefore, a precise description of any direct role for transcription in the initiation of replication must await further biochemical and ultrastructural study.

We thank the Wellcome Trust (A.B.H.), the E. P. Abraham Research Fund (R.E.) and the Cancer Research Campaign (P.R.C., D.A.J.) for support, Dr D. Shotton for use of the confocal microscope and Drs D. Vaux and M. Fricker for help with data manipulation.

## REFERENCES

- Adolph, S., Brusselbach, S. and Muller, R. (1993). Inhibition of transcription blocks cell cycle progression of NIH3T3 fibroblasts specifically in G<sub>1</sub>. *J. Cell Sci.* **105**, 113-122.
- Ahnert-Higler, G., Mach, W., Fohr, K. J. and Gratzl, M. (1989). Poration by a  $\alpha$ -toxin and streptolysin O: an approach to analyze intracellular processes. *Meth. Cell Biol.* **31**, 63-90.
- Carmo-Fonseca, M., Ferreira, J. and Lamond, A. I. (1993). Assembly of sn RNP-containing coiled bodies is regulated in interphase and mitosis - evidence that the coiled body is a kinetic nuclear structure. *J. Cell Biol.* **120**, 841-852.
- Carter, K. C., Bowman, D., Carrington, W., Fogarty, K., McNeil, J. A., Fay, F. S. and Lawrence, J. B. (1993). A three-dimensional view of precursor messenger RNA metabolism within the nucleus. *Science* **259**, 1330-1335.
- Cook, P. R. (1991). The nucleoskeleton and the topology of replication. *Cell* **66**, 627-635.
- Cox, R. F. (1976). Quantitation of elongating form A and B RNA polymerases in chick oviduct nuclei and effects of estradiol. *Cell* **7**, 455-465.
- Edgar, B. A. and Schubiger, G. (1986). Parameters controlling transcriptional activation during early *Drosophila* development. *Cell* **44**, 871-877.
- Hassan, A. B. and Cook, P. R. (1993). Visualization of replication sites in unfixed human cells. *J. Cell Sci.* **105**, 541-550.
- Hatton, K. S., Dhar, V., Brown, E. H., Iqbal, M. A., Stuart, S., Didamo, V. T. and Schildkraut, C. L. (1988). Replication program of active and inactive multigene families in mammalian cells. *Mol. Cell Biol.* **8**, 2149-2158.
- Heintz, H. H. (1992). Transcription factors and the control of DNA replication. *Curr. Opin. Cell Biol.* **4**, 459-467.
- Hozák, P., Hassan, A. B., Jackson, D. A. and Cook, P. R. (1993). Visualization of replication factories attached to a nucleoskeleton. *Cell* **73**, 361-373.
- Jackson, D. A. and Cook, P. R. (1986b). A cell-cycle dependent DNA polymerase activity that replicates intact DNA in chromatin. *J. Mol. Biol.* **192**, 65-76.
- Jackson, D. A. and Cook, P. R. (1986a). Replication occurs at a nucleoskeleton. *EMBO J.* **5**, 1403-1410.
- Jackson, D. A. and Cook, P. R. (1988). Visualization of a filamentous nucleoskeleton with a 23nm axial repeat. *EMBO J.* **7**, 3667-3677.
- Jackson, D. A., Yuan, J. and Cook, P. R. (1988). A gentle method for preparing cyto- and nucleo-skeletons and associated chromatin. *J. Cell Sci.* **90**, 365-378.
- Jackson, D. A., Hassan, A. B., Errington, R. J. and Cook, P. R. (1993). Visualization of focal sites of transcription within human nuclei. *EMBO J.* **12**, 1059-1065.
- Kill, I. R., Bridger, J. M., Cambell, K. H. S., Maldonado-Codina, G. and Hutchison, C. J. (1991). The timing of the formation and usage of replicase clusters in S-phase nuclei of human diploid fibroblasts. *J. Cell Sci.* **100**, 869-876.
- Kornberg, A. and Baker, T. (1992). *DNA Replication*, 2nd edition. W.H. Freeman, New York.
- Manders, E. M. M., Verbeek, F. J. and Aten, J. A. (1993). Measurement of co-localization of objects in dual-colour confocal images. *J. Microsc.* **169**, 375-382.
- Mills, A. D., Blow, J. J., White, J. G., Amos, W. B., Wilcock, D. and Laskey, R. A. (1989). Replication occurs at discrete foci spaced throughout nuclei replicating in vitro. *J. Cell Sci.* **94**, 471-477.
- Nakamura, H., Morita, T. and Sato, C. (1986). Structural organisation of replicon domains during DNA synthetic phase in the mammalian nucleus. *Exp. Cell Res.* **165**, 291-297.
- Nakayasu, H. and Berezney, R. (1989). Mapping replication sites in the eukaryotic cell nucleus. *J. Cell Biol.* **108**, 1-11.
- Newport, J. and Kirschner, M. (1982). A major developmental transition in early *Xenopus* embryos: II. Control of the onset of transcription. *Cell* **30**, 687-696.
- O'Keefe, R. T., Henderson, S. C. and Spector, D. L. (1992). Dynamic organization of DNA replication in mammalian cell nuclei: spatially and temporally defined replication of chromosome-specific  $\alpha$ -satellite sequences. *J. Cell Biol.* **116**, 1095-1110.
- Sambrook, J., Fritsch, E. F. and Maniatis, T. (1989). *Molecular Cloning*. 2nd edition. Cold Spring Harbor Laboratory Press, New York.
- Shaw, P., Hightett, M. and Rawlings, D. (1992). Confocal microscopy and image processing in the study of plant nuclear structure. *J. Microsc.* **166**, 87-97.
- Taneja, K. L., Lifshitz, L. M., Fay, F. S. and Singer, R. H. (1992). Poly(A) RNA codistribution with microfilaments: evaluation by in situ hybridization and quantitative digital imaging microscopy. *J. Cell Biol.* **119**, 1245-1260.
- Vourc'h, C., Taruscio, D., Boyle, A. L. and Ward, D. L. (1993). Cell cycle-dependent distribution of telomeres, centromeres, and chromosome-specific subsatellite domains in the interphase nucleus of mouse lymphocytes. *Exp. Cell Res.* **205**, 142-151.
- Wansink, D. G., Schul, W., van der Kraan, I., van Steensel, B., van Driel, R. and de Jong, L. (1993). Fluorescent labelling of nascent RNA reveals transcription by RNA polymerase II in domains scattered throughout the nucleus. *J. Cell Biol.* **122**, 283-293.
- Waseem, N. H. and Lane, D. P. (1990). Monoclonal antibody analysis of the proliferating cell nuclear antigen (PCNA): structural conservation and detection of a nucleolar form. *J. Cell Sci.* **96**, 121-129.
- Xing, Y., Johnson, C. V., Dobner, P. R. and Lawrence, J. B. (1993). Higher level organization of individual gene transcription and RNA splicing. *Science* **259**, 1326-1330.